Macromolecules

pubs.acs.org/Macromolecules Article

Quantitative Validation of the Living Coordinative Chain-Transfer Polymerization of 1-Hexene Using Chromophore Quench Labeling

Eric S. Cueny, Lawrence R. Sita, and Clark R. Landis*

Cite This: *Macromolecules* 2020, 53, 5816−5825 Read Online

ACCESS | Metrics & More | Article Recommendations | Supporting Information

ABSTRACT: In this report, we apply the chromophore quench-labeling (CQL) technique to living, homogeneous polymerization catalysts and living coordinative chain-transfer polymerization (LCCTP) conditions. We observe 100% active site counts via CQL for 1-hexene polymerization as catalyzed by two different cyclopentadienyl amidinate (CPAM) group 4 metal complexes, both previously reported to be living polymerization catalysts. We obtain a rate constant for the propagation of 1-hexene catalyzed by the CPAM hafnium complex. Selective iodinolysis and ^{1}H NMR analysis of polymer chain ends enable the quantification of Zn−polymeryls; at low conversions (∼10% conversion), nearly 2 polymer chains per Zn are observed. Through Mayo analysis and kinetic simulations, we estimate the rate of Hf−polymeryl for Zn−ethyl exchange in polymerization. Beyond active site counting, the chromophore quench-labeling method enables the observation of catalyst-bound polymeryl molecular mass distributions (MMDs) using gel permeation chromatography (GPC) with an inline UV detector (UV-GPC). Comparison of the MMDs of catalyst-bound polymeryls and all polymer chains (measured using refractive index detection, RI-GPC) reveals important mechanistic details. With the exception of early time points in the reaction, we observe excellent overlap between the UV-GPC and the RI-GPC traces. These results reveal that equilibration of polymer chains on Hf and Zn occurs rapidly in the LCCTP of 1-hexene using the CPAM hafnium complex as the catalyst and diethyl zinc as the chain-transfer agent. Kinetic simulations indicate that the Hf−polymeryl for Zn−polymeryl exchange leads to the good overlap between UV-GPC and RI-GPC traces and a crude estimate for the rate constant of this process.

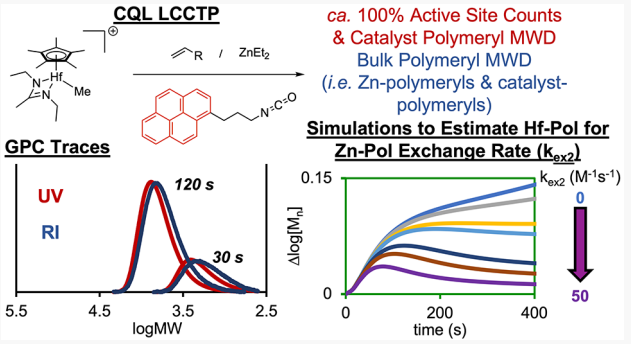

Downloaded via UNIV OF MARYLAND COLG PARK on March 13, 2021 at 10:51:12 (UTC).
See https://pubs.acs.org/sharingguidelines for options on how to legitimately share published articles.

INTRODUCTION

Polyalkenes are produced on a scale of greater than 100 million tons per year;[1] making polymerization catalysis significant to society. Polymer properties depend on many factors that include the nature of the monomer, molar mass (MM), dispersity index ($Đ$), stereotacticity, microstructure, and comonomer content of the polymer.[2,3] In this regard, the living coordinative polymerization (LCP) of alkenes, in which chain growth (propagation) proceeds in the absence of *irreversible* chain termination, offers the opportunity to design and explore new fundamental types of polyalkenes. The polyalkenes produced via LCP are uniquely defined as having a tunable number-average degree of polymerization (DP_n), a very small polydispersity index, $Đ$ (= M_w/M_n), of ≲1.1, and a wide range of accessible well-defined copolymer architectures, including random, gradient, block, graft, and comb microstructures.[4,5]

A critical issue for LCP is the "one-chain-per-active-site" relationship that exists for all polymerizations, which places a severe restriction on the ability to produce practical and scalable quantities of the final polyalkene product due to the active site being derived from exotic and expensive transition-metal initiators vis-à-vis simple organolithium reagents used as initiators for anionic living polymerizations.[6−10] Accordingly, solutions to the one-chain-per-active site liability of the LCP of alkenes are required if these new types of polyalkenes are going to successfully transition from laboratory curiosities to new technological innovations and commercial products.

Since 2000, the Sita group has been developing dimethyl cyclopentadienyl, amidinate (CPAM) group 4 metal complexes of general structure (η^5-C_5R_5)[N(R^1)C(R^2)N(R^3)]M-(CH_3)$_2$ (M = Ti, Zr, Hf) (**I**), and in particular, the C_1-symmetric Zr and C_s-symmetric Hf derivatives **1** and **2**, respectively, shown in Figure 1, as preinitiators for the (stereoselective) LCP of ethene, propene, linear and branched 1-alkenes, α,ω-nonconjugated dienes, and cycloalkenes.[1a,11−14] More importantly, since 2008, the Sita group has documented the successful development of *living coordinative chain-transfer*

Received: March 9, 2020
Revised: June 5, 2020
Published: July 15, 2020

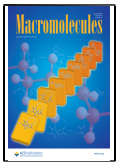

© 2020 American Chemical Society

https://dx.doi.org/10.1021/acs.macromol.0c00552
Macromolecules 2020, 53, 5816−5825

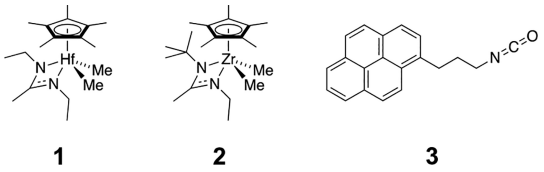

1 2 3

Figure 1. Cyclopentadienyl amidinate (CPAM) hafnium and zirconium preinitiators, **1** and **2**, respectively, and pyrenyl isocyanate quench-labeling reagent (**3**).

polymerization (LCCTP) for this same range of alkene monomers as a means to obtain practical and scalable quantities of a large variety of new fundamental types of polyalkene materials while maintaining all of the desired features of a traditional living polymerization.[1,15,16]

As Scheme 1 reveals, at the core of LCCTP is a dynamic reversible polymeryl group transfer process that occurs between a small population of transition-metal active sites derived from **1** upon "activation" using a stoichiometric amount of a borate co-initiator, such as $[PhNH(Me)_2][B(C_6F_5)_4]$, and a much larger population of "surrogate" main-group-metal chain-growth centers derived from an excess (relative to **1**) of a relatively inexpensive commodity main-group-metal alkyl, such as diethylzinc, $ZnEt_2$ (DEZ), triethylaluminum, $AlEt_3$ (TEAL), or mixtures of the two.[17,18] If the rate constant for reversible chain transfer, ν_{CT} (k_{CT}), is much larger than the rate constant for propagation, ν_p (k_p), then the populations of active and surrogate sites will appear to propagate at the same rate with the final degree of polymerization being defined by $DP_n = \{[\text{monomer}]_0 - [\text{monomer}]_t\}/([(M_A - P_A)^+ + n(M'_B - P_B)]_0)$, where n is the number of equivalent polymeryl groups per main-group metal (e.g., $n = 2$ for DEZ) and $Đ \approx 1 + k_p/k_{CT}$.[15−17] Another advantage of LCCTP over traditional LCP is that the final main-group-metal polymeryl product can be further functionalized to produce poly(α-olefinates) (xPAOs) products through simple chemical transformations involving the reactive Zn−C (or Al−C) bonds.[19]

Gibson and co-workers first demonstrated the use of DEZ as a chain-transfer agent (CTA) in the *controlled* coordinative chain-transfer polymerization (CCTP) of ethene.[20,21] To date, several different CTAs have been reported for CCTP including aluminum alkyls,[21−26] magnesium alkyls,[27−30] and zinc alkyls.[15,16,20,21,31,32] Transalkylation between the transition-metal-bound polymer chains and CTAs is believed to occur through a four-membered intermediate as shown in Figure 2.[33] The rates of chain transfer are controlled by the stability of this intermediate relative to the monomeric catalyst and chain-transfer species.[21,31,34,35] If the intermediate is thermodynamically more stable than separated CTA and catalyst, then propagation will be slowed via a decrease in the active, monomeric polymerization catalyst concentration.[34,36,37] Conversely, if the intermediate is too high in energy, transalkylation will be slow.[31] Thus, a narrow window exists for successful CCTP. Landis and co-workers have shown that even subtle steric differences near the catalyst and CTA have a significant impact on the rates of chain transfer. For example, in the Hf−pyridyl amido-catalyzed homopolymerization of 1-octene, exchange between a Hf−polyoctene chain and $ZnMe_2$ is faster than that with $ZnEt_2$ and reverse chain transfer (i.e., Hf−polyoctenyl for Zn−polyoctenyl exchange) does not occur at detectable levels.[38,39] The exchange between Hf−polyoctenyl chains and Zn−ethyls is faster than that between Hf−polyoctenyl chains and Al−ethyls; neither $ZnEt_2$ nor $AlEt_3$ inhibits propagation (though $AlEt_3$ does inhibit initiation of the Hf−pyridyl amido catalyst).[38−40] In the Hf−pyridyl amido-catalyzed copolymerization of ethene and 1-octene, Hf−polymeryl for Zn−polymeryl exchange does occur; the presence of ethene adjacent to the catalyst/CTA reduces the steric barrier to transalkylation.[41] These results represent the difficulty in developing successful CCTP because subtle changes can have significant impacts on the rates of chain transfer. In light of these difficulties, the apparently high efficiency for fast, reversible chain transfer reported by Sita and co-workers in the LCCTP of 1-alkenes using **1** and DEZ to obtain practical quantities of "precision" polyolefin materials of tunable DP_n and very narrow polydispersity stands out as being quite unique in the field.[15−17] To date, the mechanistic proposal of Scheme 1 for LCCTP has not been experimentally probed with respect to quantification of the polymeryl group transfer efficiency between active and surrogate species.

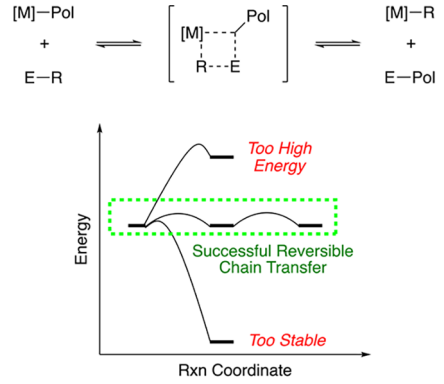

Figure 2. Mechanism of chain transfer and generic free energy surface for chain transfer between an active polymerization catalyst ([M]) and the chain-transfer reagent (E), where R is either an alkyl or a polymeryl species. Boxed in green is the ideal scenario for rapid and reversible chain transfer without inhibition of polymerization.

Chromophore quench-labeling (CQL) techniques developed by Landis and co-workers enable detailed kinetic investigations of catalytic alkene polymerization reactions.[39,42] CQL effects selective, covalent tagging of catalyst-bound

Scheme 1. Living Coordinative Chain-Transfer Polymerization (LCCTP)

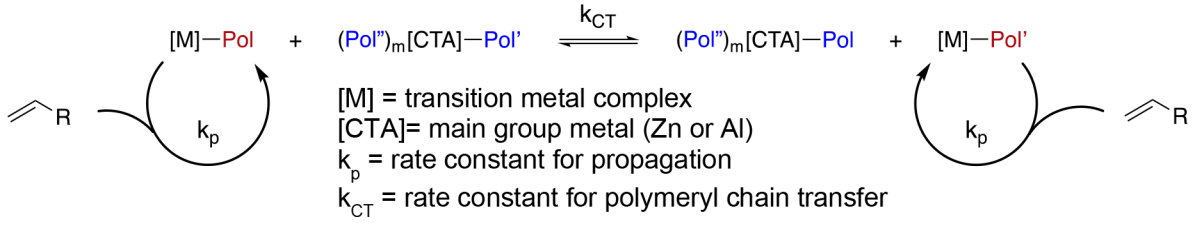

https://dx.doi.org/10.1021/acs.macromol.0c00552
Macromolecules 2020, 53, 5816−5825

polymer chains with a UV chromophore through addition of the quench-labeling reagent **3** (Figure 1). Analysis of the quenched polymers using gel permeation chromatography (GPC) with inline UV and RI detectors (UV- and RI-GPC) yields molar mass distribution (MMD) data, at the time of quench, for (1) the polymer chains attached to the catalyst (UV detector) and (2) all chains in solution (RI detector). Integration of the UV signal provides the total number of catalyst-bound polymeryls, or active site count, of the polymerization. Because **3** does not react with Zn−alkyls, catalyst-selective quench labeling can be performed in the presence of Zn polymeryls. Because refractive index (RI) detection reveals the MMD of all polymer chains, comparisons between the UV-GPC (catalyst-bound polymeryls) and RI-GPC (all polymeryls) traces yield key mechanistic information.

Herein, we report the results of an investigation into the LCP of 1-hexene using the preinitiator **2** and of the LCCTP of this monomer using **1** and DEZ as CTA as interrogated by quantitative CQL end-group analysis. First, we establish that successful, quantitative quench labeling can be achieved using quench-labeling reagent **3** in the **2**-catalyzed polymerization of 1-hexene. We then apply quench labeling to the **1**-catalyzed 1-hexene polymerization in the presence of $ZnEt_2$ (LCCTP conditions). Next, we examine the rate of chain transfer using Mayo analyses, selective iodinolysis of Zn−polymeryls with quantification by ^1H NMR spectroscopy, and kinetic simulations. Last, we use kinetic simulations to demonstrate how Hf−polymeryl for Zn−polymeryl exchange leads to increasing overlap between the UV- and the RI-GPC traces with reaction time. These results demonstrate, in relatively few experiments, a collection of significant kinetic and mechanistic information for polymerization processes. Gratifyingly, these results validate the remarkably high efficiency for reversible chain transfer in the LCCTP of 1-alkenes using CPAM initiators when carried out under previously reported conditions.

RESULTS AND DISCUSSION

CQL Results for 2-Catalyzed Polymerization of 1-Hexene Indicate Living Polymerization Behavior. We examined polymerization of 1-hexene as catalyzed by **2** at −10 °C and quenched the reaction with **3** after 2 h (see Supporting Information for details). Observations include narrow MMDs ($Đ$ < 1.1), good matches between the UV- and the RI-GPC traces (Figure 3), and 98 ± 9% active site counts as revealed by integration of the UV-GPC signal (i.e., all of the added catalyst has a polymer chain bound to the metal center that is covalently labeled by **3**). Calculation of the catalyst concentration based on the number average molecular mass (M_n) of the polyhexene and the molar ratio of consumed monomer to added catalyst is consistent with 100% active sites (see Supporting Information for details). Use of excess **3** in quench labeling yields the same active site counts. Together, these data strongly support two conclusions: (1) **2** is a truly living polymerization catalyst under the conditions studied and (2) **3** works as a quantitative quench-labeling reagent with a living polymerization catalyst. Thus, these results reinforce previous claims that **2** is a living catalyst and that **3** is a quantitative quench-label reagent.

Active Site Counts and Propagation Rates for the 1-Catalyzed Polymerization of 1-Hexene. With the results from catalyst **2** in hand, we turned to quench labeling **1** in the presence of $ZnEt_2$ (LCCTP conditions). We first established

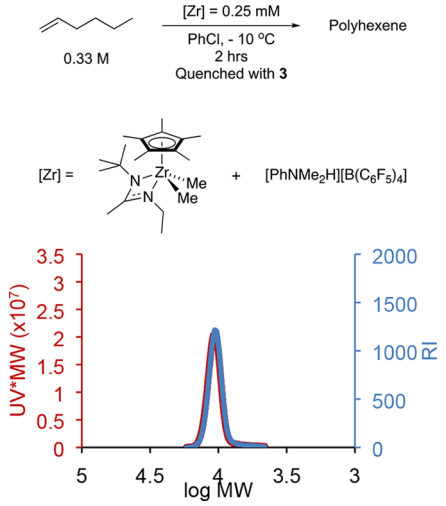

Figure 3. **2**-Catalyzed living polymerization of 1-hexene.

the temporal profile of monomer consumption in the LCCTP of 1-hexene catalyzed by **1** at two different $ZnEt_2$ concentrations (Figure 4). Under LCCTP conditions,

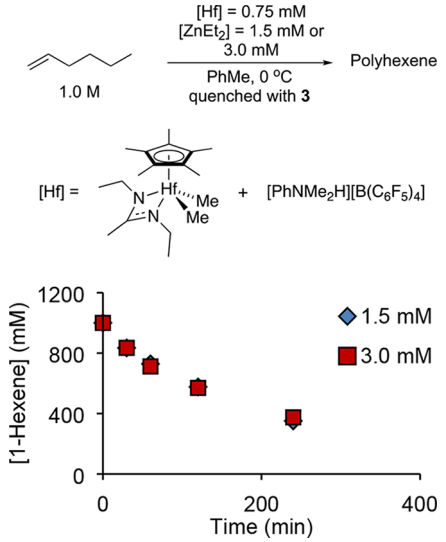

Figure 4. 1-Hexene polymerization catalyzed by **1** under LCCTP conditions in the presence of two different $ZnEt_2$ concentrations (3.0 or 1.5 mM).

initiation is fast relative to propagation as revealed by the lack of an induction period in the consumption of 1-hexene. The active site counts are ∼100% throughout the time course of polymerization, and the polymerization rate is independent of the $ZnEt_2$ concentration. On the basis of the monomer consumption and active site counts, the rate constant for propagation for **1** at 0 °C is determined to be k_p = 0.103 ± 0.005 M^{-1} s^{-1} (see Supporting Information for details).

Chain Transfer between 1 and $ZnEt_2$ in the Polymerization of 1-Hexene. With the rate of propagation established, we examined the rate of exchange between Hf and Zn using a Mayo analysis.[38,43,44] Polymerizations of 1-hexene were conducted using catalyst **1** at different $ZnEt_2$ concentrations; reactions were quenched at ∼10% conversion of 1-hexene (30 min polymerization time) using **3**. The MMDs of polyhexene produced at different $ZnEt_2$ concentrations are

https://dx.doi.org/10.1021/acs.macromol.0c00552
Macromolecules 2020, 53, 5816−5825

shown in Figure 5a. Mayo plots were constructed by plotting $1/M_n$ vs $[ZnEt_2]_0/(84.16 \times [1\text{-hexene}]_0)$; the gradient of this

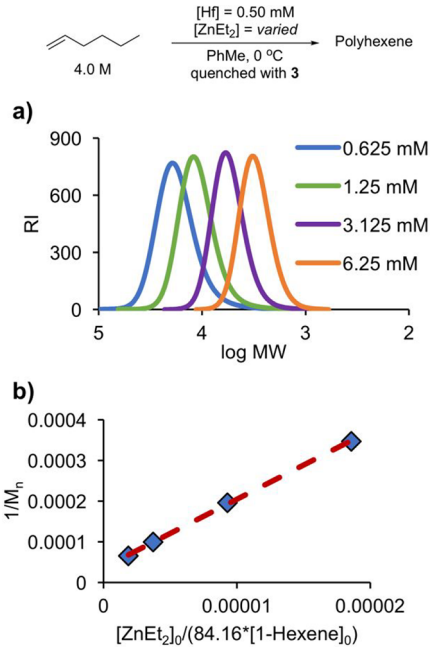

Figure 5. Polymerization of 1-hexene catalyzed by **1** in the presence of varying initial concentrations of $ZnEt_2$. (a) MMD of polyhexene produced after 30 min (~10% conversion) at different $ZnEt_2$ concentrations. (b) Mayo plot of $1/M_n$ vs $[Zn]_0/(84.16 \times [1\text{-hexene}]_0)$.

plot represents the *apparent* exchange to propagation ratio, $k_{ex}/k_p = 16.8 \pm 0.1$ (Figure 5b). Upon the basis of the rate of propagation (vide supra), the rate constant for exchange is 1.7 M^{-1} s^{-1}.

Previously, Sita and co-workers established that two polymer chains per Zn are produced upon complete consumption of monomer in the **1**-catalyzed LCCTP.[17] However, it is unclear at what point in the polymerization two polymer chains per Zn are produced. Previously, Landis and co-workers found that for the Hf–pyridyl amido-catalyzed homopolymerization of 1-octene only one polymer chain per Zn is produced;[38] however, in the copolymerization of ethene and 1-octene nearly two polymer chains per Zn are produced.[41] These results raise the question at low conversion how many polymer chains per Zn are generated in the **1**-catalyzed polymerization of 1-hexene?

To quantify the number of polymer chains produced per Zn, we performed iodinolysis of Zn–polymeryls followed by ^{1}H NMR analysis of polymer chain ends. These experiments were conducted by quenching the polymerizations with **3** after 30 min (~10% conversion of 1-hexene), which selectively reacts with the catalyst-bound polymeryls, then adding I_2 to react with the Zn–polymeryls quantitatively generating I–polymeryl species that are measured by ^{1}H NMR spectroscopy. These experiments demonstrate that nearly two polymer chains per Zn are produced within the first ~10% conversion of 1-hexene at two different concentrations of $ZnEt_2$ (Table 1).

Because nearly two polymer chains per Zn are produced at low conversion (~10%) of 1-hexene, we conclude that the first ethyl exchange (Hf–polymeryl for Zn(Et)–ethyl exchange) and second ethyl exchange (Hf–polymeryl for Zn(polymeryl)–ethyl exchange) are both fast relative to

Table 1. Number of Polymer Chains Produced per Zn[a]

$[ZnEt_2]_0$ (mM)	polymer chains per Zn
1.25	1.9 ± 0.1
6.25	1.8 ± 0.1

[a]The number of polymer chains determined through iodinolysis of Zn–polymeryl species with subsequent ^{1}H NMR analysis of polymer chain ends. Conditions: [**1**] = 0.50 mM, $[PhNMe_2H][B(C_6F_5)_4]$ = 0.50 mM, $[1\text{-hexene}]_0$ = 4.0 M, in toluene (1 mL) at 0 °C quenched with 2 equiv of **3** after 30 min.

propagation and are similar to each other. Thus, it is unlikely that these studies will be able to distinguish between the first and the second Zn–ethyl exchange rates. Furthermore, because nearly two polymer chains per Zn are produced prior to conducting the Mayo analysis, it is possible that the slope of the Mayo plot has contributions from exchange between Zn–polymeryls and Hf–polymeryls as well. For clarity we refer to the slope of the Mayo plot as the *apparent* exchange rate constant (k_{exapp}), hence, k_{exapp} = 1.7 M^{-1} s^{-1}.

Kinetic Simulations To Better Understand Transalkylation between Hf and Zn. To better understand the effect of different exchange processes on polymer MMDs, we simulated 1-hexene polymerization as catalyzed by **1** in the presence of $ZnEt_2$. The kinetic model for LCCTP (Scheme 2)

Scheme 2. Model for 1-Catalyzed 1-Hexene Polymerization[a]

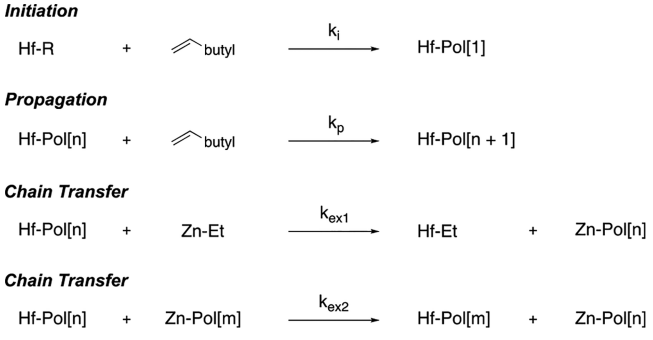

[a]R = Me or Et. The Hf–Et is produced following chain transfer between a Zn–Et and a Hf–Pol, whereas the Hf–Me is derived from the precatalyst. Because initiation is fast, relative to propagation, Hf–Me and Hf–Et are treated identically. All Hf species are cationic.

involves propagation (k_p), Hf–polymeryl for Zn–ethyl exchange (k_{ex1}), and Hf–polymeryl for Zn–polymeryl exchange (k_{ex2}). For simplicity, we set the initiation rate constant (k_i) to a large value because the data show no induction effects and assumed that the rate constants for Hf–polymeryls exchanging with Zn(Et)–ethyl and Zn(polymeryl)–ethyl are the same (k_{ex1}). The rate constant for exchange of Zn–polymeryls with Hf–polymeryls is labeled k_{ex2}. Using the previously determined rate constant of propagation (k_p = 0.103 M^{-1} s^{-1}) and various values of k_{ex1} and k_{ex2} we examined the simulated temporal profile of $ZnEt_2$ conversion to Zn–polymeryls (Figure 6a).

The kinetic model of Scheme 2 is consistent with the experimental Mayo analysis. Figure 6 summarizes the results of kinetic simulations of $ZnEt_2$ conversion for different k_{ex1} values. Unsurprisingly, the value of k_{ex1} has a significant impact on the consumption of $ZnEt_2$ during polymerization. Increasing k_{ex1} beyond ~3.4 M^{-1} s^{-1} leads to complete conversion of all Zn–

https://dx.doi.org/10.1021/acs.macromol.0c00552
Macromolecules 2020, 53, 5816−5825

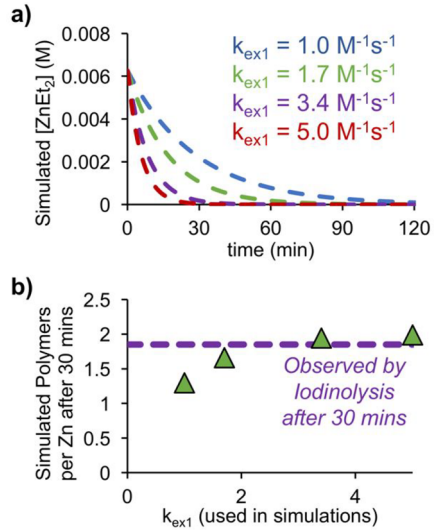

Figure 6. (a) Simulated temporal profile of the concentration of $ZnEt_2$ in the **1**-catalyzed 1-hexene polymerization at various values of k_{ex1}. (b) Number of polymer chains per Zn after 30 min based on the kinetic simulations vs the value of k_{ex1} (green triangles), and number of polymer chains observed via iodinolysis experiments (purple dashed line).

Et groups to Zn−polymeryls at the 30 min time point. The number of polymer chains per Zn at 30 min plotted against the value of k_{ex1} (Figure 6b) matches the experimentally observed polymer chains per Zn (1.9, determined by iodinolysis experiments) for k_{ex1} > ca. 3.4 M^{-1} s^{-1}.

Variation of the Zn−polymeryl/Hf−polymeryl exchange rate constant, k_{ex2}, has no impact on the rate of $ZnEt_2$ conversion nor any significant effect on the value of M_n. Figure 7 depicts the evolution of the average polymer mass

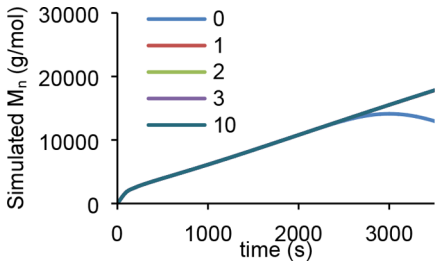

Figure 7. Simulation of the M_n at different values of k_{ex2} using the kinetic model shown in Scheme 2. For this simulation, $[Hf-R]_0$ = 0.58 mM, $[1\text{-hexene}]_0$ = 4.0 M, $[Zn-Et]_0$ = 3.0 mM, k_p = 0.103 M^{-1} s^{-1}, k_{ex1} = 3.7 M^{-1} s^{-1}, and k_{ex2} values of 0−10 M^{-1} s^{-1} are examined.

with time according to simulations with k_{ex1} = 3.7 M^{-1} s^{-1} and different values of k_{ex2}. Over a 60 min time period (corresponding to 30% monomer conversion), only k_{ex2} = 0 affects the predicted M_n values for the range of k_{ex2} values that were examined.

Ratios of exchange to propagation rates as estimated by Mayo analysis can depend on the reaction time (or monomer conversion) at which the experimental data are collected. We examined the impact of shorter reaction times on Mayo analyses for experimental measurements of **1**-catalyzed LCCTP of 1-hexene at varying concentrations of $ZnEt_2$. We chose 5 min reaction time because simulations of $ZnEt_2$ concentration with time (Figure 6a) indicate incomplete consumption of $ZnEt_2$ at this time. The Mayo analysis conducted after 5 min yields a 2-fold higher exchange to propagation ratio (k_{exapp}/k_p = 36.2 ± 0.8) than the previous Mayo analysis at 30 min reaction time (k_{exapp}/k_p = 16.8 ± 0.1). As discussed, the major discrepancy between these Mayo analyses (5 min vs 30 min reaction time) is concentration of unmodified $ZnEt_2$. After 30 min essentially no $ZnEt_2$ remains, and exchange processes are limited to Zn−polymeryl/Hf−polymeryl exchange. On the basis of the Mayo analysis conducted after 5 min, the estimated rate constant for Hf−polymeryl/Zn−ethyl exchange (k_{ex1}) is 3.7 M^{-1} s^{-1}. This rate constant, according to kinetic simulations, would result in ∼1.9 polymer chains per Zn being produced after 30 min of polymerization (Figure 6b), matching the number of polymer chains per Zn observed via iodinolysis.

Why Do the Results of the Mayo Analysis Depend on the Reaction Time? According to simulations, the M_n is primarily influenced by the value of k_{ex1}; this is due to the relative differences in MW (ΔM_n) of exchanging alkyl groups between the catalyst and CTA. The exchange of Hf−polymeryls and Zn−ethyls (k_{ex1} Scheme 2) has the largest impact on the observed M_n because polymeryls and ethyls have a large ΔM_n. The k_{ex2} value has little influence on M_n because the ΔM_n is relatively small between the Hf−polymeryl and the Zn−polymeryl chains.

While the k_{ex2} does not impact M_n, it does affect the M_w and therefore the dispersity ($Đ$). The value of $Đ$ is larger at low conversion because the ΔM_n between the Hf and the Zn species is the largest when the Zn species are all $ZnEt_2$. The ΔM_n between the Hf−polymeryls and the Zn−alkyls decreases over the course of the reaction, becoming infinitely small at long reaction times. Such small ΔM_n for Hf− and Zn−polymeryls leads to the narrow MMDs ($Đ$ < 1.1) observed by Sita and co-workers in the LCCTP.

The *apparent* exchange to propagation ratio determined by Mayo analysis is influenced by the speciation of Zn−alkyls during polymerization. Early in the reaction, most of the Zn−alkyls are Zn−ethyls; as polymerization continues (and chain transfer occurs), the Zn−ethyls are converted to Zn−polymeryls. The change in the speciation of Zn−alkyls (from Zn−ethyl to Zn−polymeryl) alters the M_n for all polymers in solution, thus influencing the *apparent* exchange to propagation ratio.

Due to the discrepancies in the observed exchange to propagation ratio obtained by Mayo analyses conducted at different reaction times, we chose to simulate the exchange to propagation ratio at different reaction times to better understand the influence of conversion on the Mayo analysis. The model used for these simulations is shown in Scheme 2 using the rate constants k_p = 0.103 M^{-1} s^{-1}, k_{ex1} = 3.7 M^{-1} s^{-1}, and k_{ex2} = *varied* (details can be found in the Supporting Information). Through these simulations, we established that the exchange to propagation ratio decreases throughout the polymerization. However, prior to 50% conversion of Zn−ethyls to Zn−polymeryls the exchange to propagation ratio estimated by Mayo analysis is constant (Figure 8). After 50% conversion of Zn−ethyls to Zn−polymeryls, the exchange to propagation ratio decreases with increasing conversion of Zn−ethyls to Zn−polymeryls. The value of k_{ex2} has no influence on the exchange to propagation ratio prior to complete conversion of Zn−ethyls to Zn−polymeryls. Thus, these simulations lend further support to the notion that the speciation of the CTA significantly impacts the Mayo analysis. However, prior to 50%

https://dx.doi.org/10.1021/acs.macromol.0c00552
Macromolecules 2020, 53, 5816−5825

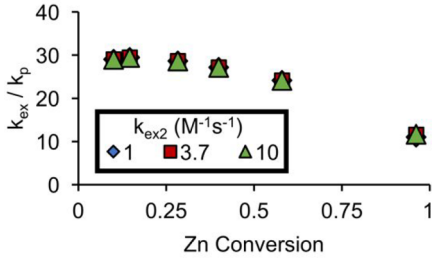

Figure 8. k_{ex}/k_p determined through kinetic simulations plotted vs the conversion of Zn−ethyls to Zn−polymeryls. Kinetic model for these simulations is shown in Scheme 2. Conditions: $[Hf-R]_0$ = 0.0005 M, $[1\text{-hexene}]_0$ = 4.0 M, k_p = 0.103 M^{-1} s^{-1}, k_{ex1} = 3.7 M^{-1} s^{-1}, concentration of CTA was varied, and k_{ex2} was also varied. For details on the performance of these kinetic simulations, see the Supporting Information.

conversion of Zn−ethyls to Zn−polymeryls, the exchange to propagation ratio gives a fairly accurate description of the Hf−polymeryl for the Zn−ethyl exchange rate (k_{ex1}).

Comparison of the UV- and RI-GPC Traces. An advantage of the CQL technique is that the UV and RI traces probe different polymeryl distributions (Hf bound vs all polymers) at the time of quench. The experimental MMDs of polyhexene produced after 30 and 5 min of polymerization are somewhat broadened ($Đ \approx 1.2-1.3$) compared to previous results by Sita and co-workers ($Đ < 1.1$).[15,16] However, the results of Sita and co-workers were at longer reaction times (full conversion of monomer) and/or higher $ZnEt_2$ concentrations (relative to catalyst concentration). For the studies reported herein, at 30 min reaction time the RI- and UV-GPC traces of these polymerization reactions are nearly identical (see Supporting Information). The fairly narrow MMDs (Table 2) and good overlap between UV- and RI-GPC traces

Table 2. M_n and $Đ$ after 5 min of Polymerization with Different $ZnEt_2$ Concentrations[a]

$[ZnEt_2]_0$ (mM)	M_n (kg mol^{-1})	$Đ$
0.5	15.3	1.28
1.0	10.0	1.20
2.5	5.10	1.15

[a]Conditions: [**1**] = 0.58 mM, $[PhNMe_2H][B(C_6F_5)_4]$ = 0.58 mM, $[1\text{-hexene}]_0$ = 4.0 M, toluene (1 mL), 0 °C. Quenched with **3** (2 equivalents relative to **1**) after 5 min.

strongly support the occurrence of "reversible" chain transfer (Hf−polymeryl for Zn−polymeryl exchange) as previously concluded by Sita and co-workers.

To better understand the effect of k_{ex2} on the **1**-catalyzed LCCTP of 1-hexene, we conducted polymerizations at even shorter reaction times (30−120 s) (Figure 10). At these very low conversions the MMDs are somewhat broad ($Đ \approx 1.3$). Tellingly, the UV- and RI-GPC traces (Figure 10) diverge at these early time points. The UV-GPC trace is higher in MM than the RI-GPC trace, and the overlap between the UV- and the RI-GPC traces increases with reaction time. Because **3** selectively reacts with Hf−polymeryls, the UV-GPC trace reflects the MMD of catalyst-bound polymer chains whereas the RI-GPC trace reflects the total MMD of polymer chains (catalyst-bound polymer chains and Zn−polymeryls).

As discussed previously, the ΔM_n between the Hf and the Zn species has a major impact on the MMD of polymer produced. The $Đ$ decreases over the time course of polymerization because the ΔM_n between the Hf and the Zn species decreases as chain transfer converts Zn−ethyls to Zn−polymeryls. The difference between the MMD of catalyst−polymeryls (observed through UV-GPC) and the overall MMD of polymeryls (observed through RI-GPC) is also influenced by the ΔM_n between the Hf and the Zn species. As polymerization continues, chain transfer between Hf−polymeryls and Zn−polymeryls occurs and polymer chains continue to grow from Hf via propagation. This process results in a negligible difference between the ΔM_n of the polymeryls on the catalyst and CTA; thus, the overlap between UV- and RI-GPC traces increases. These observations are in agreement with the mathematical analysis of coordinative chain-transfer polymerization conducted by Britovsek and co-workers; $Đ$ approaches unity during living polymerization reactions with fast rates of chain transfer (relative to propagation) according to eq 1, where λ = number of inserted monomers.[45] In the **1**-catalyzed LCCTP of 1-hexene, we observe increased overlap of the UV- and RI-GPC traces over the course of 30−120 s (Figure 10).

$$Đ = \frac{M_w}{M_n} = \frac{(\lambda + 1)(1 - e^{-\lambda})}{\lambda} \quad (1)$$

How Does the Rate of k_{ex2} Influence the Overlap between the UV-GPC and the RI-GPC Signals with Time? To answer this question, we examined kinetic simulations of the MMDs. In these simulations (Figure 9)

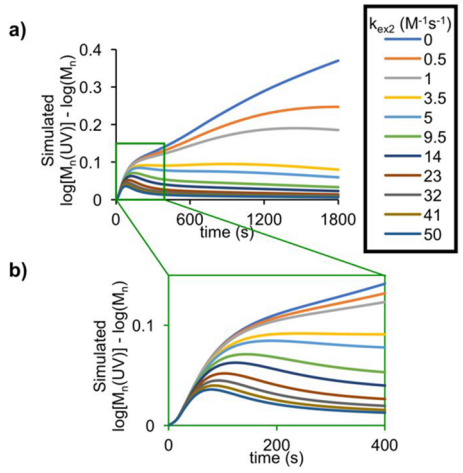

Figure 9. (a) Simulations of the difference of the M_n between the overall polymer MMD (RI) and the MMD of the catalyst-bound polymeryls (UV). Simulation of the difference in the log(M_n) of the RI and UV signals is plotted vs time at different k_{ex2} values. Kinetic model for these simulations is shown in Scheme 2. Conditions: $[Hf-R]_0$ = 0.0005 M, $[1\text{-hexene}]_0$ = 4.0 M, k_p = 0.103 M^{-1} s^{-1}, k_{ex1} = 3.7 M^{-1} s^{-1}, [ZnEt] = 0.003 M. (b) Boxed area of a.

we varied the value of k_{ex2} and plot the difference in log MM between the overall M_n and the M_n of the UV-GPC trace (i.e., M_n of the Hf−polymeryls only). The Δlog MM decreases with increasing polymerization time (when $k_{ex2} > 0$); thus, the overlap between the UV- and the RI-traces increases with increasing polymerization time. Upon increasing the value of k_{ex2}, the overlap between the UV- and the RI-traces increases more rapidly in polymerization. Without polymeryl for polymeryl exchange (i.e., $k_{ex2} = 0$), the difference between

https://dx.doi.org/10.1021/acs.macromol.0c00552
Macromolecules 2020, 53, 5816−5825

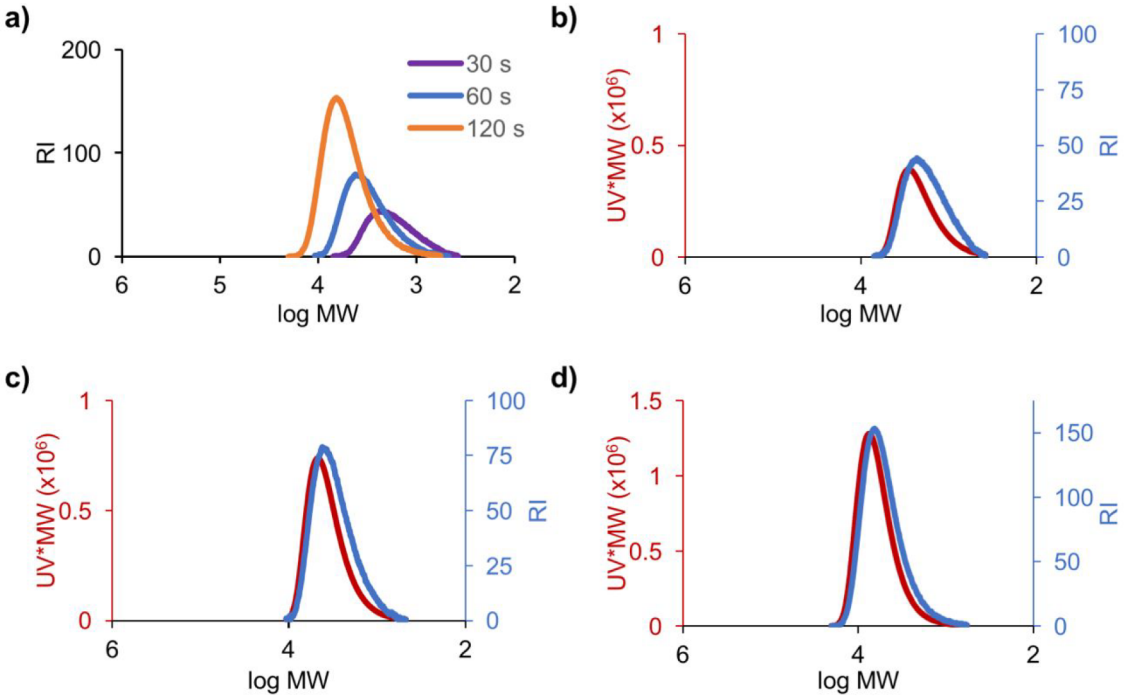

Figure 10. MMDs of polyhexene produced by **1** in the presence of $ZnEt_2$ at relatively short time points. (a) Temporal profile of RI-GPC traces in the **1**-catalyzed polymerization of 1-hexene in the presence of $ZnEt_2$ quenched with **3** after 30 (purple), 60 (blue), and 120 s (orange). (b) UV- and RI-GPC traces at the 30 s time point. (c) UV- and RI-GPC traces at the 60 s time point. (d) UV- and RI-GPC traces at the 120 s time point. Conditions: [**1**] = 0.58 mM, $[PhNMe_2H][B(C_6F_5)_4]$ = 0.58 mM, [1-hexene] = 4.0 M, $[ZnEt_2]$ = 0.5 mM, in toluene (1 mL) at 0 °C and quenched with **3** (2 equivalents relative to **1**).

the UV and the RI traces continues to increase throughout the polymerization reaction.

The experimental results clearly indicate that Hf−polymeryl for Zn−polymeryl exchange occurs during polymerization, resulting in the narrow MMDs observed in polymerization and the increasing overlap between the UV- and the RI-GPC traces with time. According to simulations, the value of k_{ex2} likely is similar to or greater than that of k_{ex1} in order for the overlap between the UV- and the RI-GPC traces to increase as early as the 30−120 s time scale (Figure 10). However, determining the exact value of k_{ex2} would require a much more detailed kinetic modeling analysis. Because of the large number of chemical species and accompanying differential equations required for this type of kinetic analysis, such a study was not undertaken at this time.

CONCLUSIONS

In this manuscript, we describe the application of CQL to living polymerization catalysts **1** and **2**. In the **2**-catalyzed polymerization of 1-hexene, we find that all of the catalyst is active in polymerization, the MMD of polyhexene is narrow, and the UV- and RI-GPC traces match. These results are expected for a truly living polymerization catalyst and match the previous work of Sita and co-workers. Thus, we conclude that chromophore quench labeling works for living polymerization catalysts, confirming the validity of this technique.

We also apply the CQL to the LCCTP of 1-hexene catalyzed by **1**. In these polymerizations, $ZnEt_2$ does not inhibit polymerization at 0 °C. For comparison, the Hf−pyridyl amido catalyst is inhibited by $ZnEt_2$ at 0 °C via formation of a heterobimetallic intermediate.[46] Because **3** does not react with $ZnEt_2$, CQL studies are suitable in LCCTP. The temporal profile of monomer consumption and active site counts are obtained by CQL. The rate constant for propagation was determined (k_p = 0.103 M^{-1} s^{-1}).

The rate of chain transfer was examined through Mayo analyses. Interestingly, we found that the exchange to propagation ratio is dependent on the reaction time. Through kinetic simulations, we determined that prior to 50% conversion of Zn−ethyls to Zn−polymeryls the Mayo analysis provides a good estimate of the catalyst−polymeryl for Zn−ethyl exchange.

Last, we probed the UV- and RI-GPC traces of polyhexene produced by **1** in the presence of $ZnEt_2$ to better assess the Hf−polymeryl for Zn−polymeryl exchange process. At very short reaction times (30−120 s), we observed differences in the UV- and RI-GPC traces. At longer reaction times (5 min or more), UV- and RI-GPC traces overlap nearly perfectly. These results indicate reversible chain transfer occurs and is a relatively fast process. Kinetic simulations examining the difference in M_n between the UV-trace and the RI-trace yield a crude estimate of the Hf−polymeryl for Zn−polymeryl exchange rate (k_{ex2}). A detailed quantitative kinetic modeling analysis of polymerization may provide the exact value of k_{ex2}, though this is outside the scope of this manuscript and is the subject of ongoing work.

This manuscript reveals that while the overall rates of each polymerization step (propagation and chain transfer) may be relatively slow, they produce polyhexene with tunable MM and narrow MMDs. The narrow MMDs even at low levels of conversion are enabled by the fast exchange to propagation ratio (k_{ex}/k_p = 36.2 ± 0.8) for **1**-catalyzed 1-hexene polymerization and relatively fast rate of Hf−polymeryl for Zn−polymeryl exchange. For comparison, in the Hf−pyridyl amido-catalyzed polymerization of 1-octene in the presence of

https://dx.doi.org/10.1021/acs.macromol.0c00552
Macromolecules 2020, 53, 5816−5825

$ZnEt_2$, k_{ex}/k_p = 7.3. Also, in the Hf−pyridyl amido-catalyzed polymerization of 1-octene, Hf−polymeryl for Zn−polymeryl exchange does not occur; however, the overall rate of propagation is much higher using the Hf−pyridyl amido catalyst than that in **1**-catalyzed polymerization. The origins of these differences are unclear but are of increasing interest toward the design of new catalyst systems.

■ ASSOCIATED CONTENT

Supporting Information

The Supporting Information is available free of charge at https://pubs.acs.org/doi/10.1021/acs.macromol.0c00552.

General experimental and kinetic simulation details, determination of the rate constant for propagation, Mayo analysis after 5 min of polymerization, kinetic simulations of the exchange to propagation ratio at different k_{ex2} values, simulations of the ΔM_n, and additional MMDs (PDF)

■ AUTHOR INFORMATION

Corresponding Author

Clark R. Landis − *Department of Chemistry, University of Wisconsin−Madison, Madison, Wisconsin 53706, United States;* orcid.org/0000-0002-1499-4697; Email: landis@chem.wisc.edu

Authors

Eric S. Cueny − *Department of Chemistry, University of Wisconsin−Madison, Madison, Wisconsin 53706, United States;* orcid.org/0000-0003-1244-2407

Lawrence R. Sita − *Department of Chemistry and Biochemistry, University of Maryland, College Park, Maryland 20742, United States;* orcid.org/0000-0002-9880-1126

Complete contact information is available at: https://pubs.acs.org/10.1021/acs.macromol.0c00552

Notes

The authors declare the following competing financial interest(s): L.R.S. has a financial interest in the university spin-out company, Precision Polyolefins, LLC (PPL). This work did not involve any PPL personnel, funding, or other resources.

■ ACKNOWLEDGMENTS

We thank Dr. Samantha Nowak for training E.S.C. in the experimental procedures for using catalysts **1** and **2**. We thank Dr. Anna Kiyanova (UW—Madison Soft Materials Characterization Laboratory) for help with GPC. We acknowledge the NSF through the University of Wisconsin Nanoscale Science and Engineering Center (DMR-0832760 and 0425880) for funding the GPC and the Soft Materials Laboratory. We acknowledge the NSF (CHE-1048642), NIH (S10 OD012245), and Paul and Margaret Bender Fund for support of the NMR facility. L.R.S. gratefully acknowledges partial support for this work that was provided by the NSF (CHE-1665421).

■ REFERENCES

(1) (a) Sita, L. R. Ex Uno Plures ("Out of One, Many"): New Paradigms for Expanding the Range of Polyolefins through Reversible Group Transfers. *Angew. Chem., Int. Ed.* **2009**, *48*, 2464−2472. (b) Wenzel, T. T.; Arriola, D. J.; Carnahan, E. M.; Hustad, P. D.; Kuhlman, R. L. Chain Shuttling Catalysis and Olefin Block Copolymers (OBCs). *Top. Organomet. Chem.* **2009**, *26*, 65−104. (c) Chen, C. Designing Catalysts for Olefin Polymerization and Copolymerizations: Beyond Electronic and Steric Tuning. *Nature Rev. Chem.* **2018**, *2*, 6−14.

(2) McKnight, A. L.; Waymouth, R. M. Group 4 ansa-Cyclopentadienyl-Amido Catalysts for Olefin Polymerization. *Chem. Rev.* **1998**, *98*, 2587−2598.

(3) Coates, G. W. Precise Control of Polyolefin Stereochemistry Using Single-Site Metal Catalysts. *Chem. Rev.* **2000**, *100*, 1223−1252.

(4) Coates, G. W.; Hustad, P. D.; Reinartz, S. Catalysts for the Living Insertion Polymerization of Alkenes: Access to New Polyolefin Architectures Using Ziegler−Natta Chemistry. *Angew. Chem., Int. Ed.* **2002**, *41*, 2236−2257.

(5) Domski, G. J.; Rose, J. M.; Coates, G. W.; Bolig, A. D.; Brookhart, M. Living alkene polymerization: New methods for the precision synthesis of polyolefins. *Prog. Polym. Sci.* **2007**, *32*, 30−92.

(6) Baskaran, D.; Müller, A. H. E. Anionic vinyl polymerization—50 years after Michael Szwarc. *Prog. Polym. Sci.* **2007**, *32*, 173−219.

(7) Young, R. N.; Quirk, R. P.; Fetters, L. J. Anionic polymerizations of non-polar monomers involving lithium. *Anionic Polymerization*; Springer Berlin Heidelberg: Berlin, Heidelberg, 1984; pp 1−90.

(8) Hadjichristidis, N.; Pitsikalis, M.; Pispas, S.; Iatrou, H. Polymers with Complex Architecture by Living Anionic Polymerization. *Chem. Rev.* **2001**, *101*, 3747−3792.

(9) Hirao, A.; Hayashi, M.; Loykulnant, S.; Sugiyama, K.; Ryu, S. W.; Haraguchi, N.; Matsuo, A.; Higashihara, T. Precise syntheses of chain-multi-functionalized polymers, star-branched polymers, star-linear block polymers, densely branched polymers, and dendritic branched polymers based on iterative approach using functionalized 1,1-diphenylethylene derivatives. *Prog. Polym. Sci.* **2005**, *30*, 111−182.

(10) Higashihara, T.; Hayashi, M.; Hirao, A. Synthesis of well-defined star-branched polymers by stepwise iterative methodology using living anionic polymerization. *Prog. Polym. Sci.* **2011**, *36*, 323−375.

(11) (a) Jayaratne, K. C.; Sita, L. R. Stereospecific Living Ziegler-Natta Polymerization of 1-Hexene. *J. Am. Chem. Soc.* **2000**, *122*, 958−959. (b) Jayaratne, K. C.; Keaton, R. J.; Henningsen, D. A.; Sita, L. R. Living Ziegler-Natta Cyclopolymerization of Nonconjugated Dienes: New Classes of Microphase-Separated Polyolefin Block Copolymers via a Tandem Polymerization/Cyclopolymerization Strategy. *J. Am. Chem. Soc.* **2000**, *122*, 10490−10491. (c) Keaton, R. J.; Jayaratne, K. C.; Henningsen, D. A.; Koterwas, L. A.; Sita, L. R. Dramatic Enhancement of Activities for Living Ziegler-Natta Polymerizations Mediated by 'Exposed' Zirconium Acetamidinate Inititators: The Isospecific Living Polymerization of Vinylcyclohexane. *J. Am. Chem. Soc.* **2001**, *123*, 6197−6198. (d) Jayaratne, K. C.; Sita, L. R. Direct Methyl Group Exchange Between Cationic Zirconium Ziegler-Natta Initiators and Their Living Polymers: Ramifications for the Production of Stereoblock Polyolefins. *J. Am. Chem. Soc.* **2001**, *123*, 10754−10755. (e) Kissounko, D. A.; Fettinger, J. C.; Sita, L. R. Structure/Activity Relationships for the Living Ziegler-Natta Polymerization of 1-Hexene by the Series of Cationic Monocyclopentadienyl Zirconium Acetamidinate Complexes, $[(\eta^5\text{-}C_5Me_5)ZrMe\{N(CH_2R)\text{-}C(Me)N(t\text{-}Bu)\}][B(C_6F_5)_4]$ (R = Me, i-Pr, t-Bu, Ph, 2-ClC_6H_4, 3-MeC_6H_4, 2,4,6-$Me_3C_6H_2$). *Inorg. Chim. Acta* **2003**, *345*, 121−129. (f) Zhang, Y.; Sita, L. R. Solid-Supported Stereospecific Living Ziegler-Natta Polymerization of α-Olefins. *Chem. Commun.* **2003**, 2358−2359. (g) Zhang, Y.; Reeder, E. K.; Keaton, R. J.; Sita, L. R. Goldilocks Effect of a Distal Substituent on Living Ziegler-Natta Polymerization Activity and Stereoselectivity within a Class of Zirconium Amidinate-Based Initiators. *Organometallics* **2004**, *23*, 3512−3520. (h) Kissounko, D. A.; Zhang, Y.; Harney, M. B.; Sita, L. R. Evaluation of $(\eta^5\text{-}C_5Me_5)Hf(R)_2$ {N(Et)C(Me)N(t-Bu)} (R = Me and i-Bu) for the Stereospecific Living and Degenerative Transfer Living Ziegler-Natta Polymerization of α-Olefins. *Adv. Synth. Catal.* **2005**, *347*, 426−432.

(12) (a) Zhang, Y.; Keaton, R. J.; Sita, L. R. Degenerative Transfer Living Ziegler-Natta Polymerization: Application to the Synthesis of

Monomodal Stereoblock Polyolefins of Narrow Polydispersity and Tunable Block Length. *J. Am. Chem. Soc.* **2003**, *125*, 9062−9069. (b) Zhang, Y.; Sita, L. R. Stereospecific Living Ziegler-Natta Polymerization via Rapid and Reversible Chloride Degenerative Transfer between Active and Dormant Sites. *J. Am. Chem. Soc.* **2004**, *126*, 7776−7777. (c) Zhang, W.; Sita, L. R. Investigation of Dynamic Intra- and Intermolecular Processes within a Tether-Length Dependent Series of Group 4 Bimetallic Initators for Stereomodulated Degenerative Transfer Living Ziegler-Natta Propene Polymerization. *Adv. Synth. Catal.* **2008**, *350*, 439−447.

(13) (a) Harney, M. B.; Zhang, Y.; Sita, L. R. Discrete, Multiblock Isotactic−Atactic Stereoblock Polypropene Microstructures of Differing Block Architectures through Programmable Stereomodulated Living Ziegler−Natta Polymerization. *Angew. Chem., Int. Ed.* **2006**, *45*, 2400−2404. (b) Harney, M. B.; Zhang, Y.; Sita, L. R. Bimolecular Control over Polypropene Stereochemical Microstructure in a Well-Defined Two-State System and a New Fundamental Form: Stereogradient Polypropene. *Angew. Chem., Int. Ed.* **2006**, *45*, 6140−6144. (c) Crawford, K. E.; Sita, L. R. Stereoengineering of Poly(1,3-methylenecyclohexane) via Two-State Living Coordination Polymerization of 1,6-Heptadiene. *J. Am. Chem. Soc.* **2013**, *135*, 8778−8781. (d) Crawford, K. E.; Sita, L. R. De Novo Design of a New Class of 'Hard-Soft' Amorphous Microphase-Separated Polyolefin Block Copolymer Thermoplastic Elastomer. *ACS Macro Lett.* **2015**, *4*, 921−925.

(14) Thompson, R. R.; Zavalij, P. Y.; Sita, L. R. Electronic Effect Rate Enhancement in the Stereoselective Living Coordinative Polymerization of α-Olefins by α,α,α-Trifluroacetamidinate-Modified Group 4 Metal CPAM^{CF3} Initiators. *Organometallics* **2019**, *38*, 213−217.

(15) (a) Zhang, W.; Sita, L. R. Highly Efficient, Living Coordinative Chain-Transfer Polymerization of Propene with $ZnEt_2$: Practical Production of Ultrahigh to Very Low Molecular Weight Amorphous Atactic Polypropenes of Extremely Narrow Polydispersity. *J. Am. Chem. Soc.* **2008**, *130*, 442−443. (b) Zhang, W.; Wei, J.; Sita, L. R. Living Coordinative Chain-Transfer Polymerization and Copolymerization of Ethene, α-Olefins, and α,ω-Nonconjugated Dienes using Dialkylzinc as "Surrogate" Chain-Growth Sites. *Macromolecules* **2008**, *41*, 7829−7833.

(16) (a) Wei, J.; Zhang, W.; Wickham, R.; Sita, L. R. Programmable Modulation of Co-monomer Relative Reactivities for Living Coordination Polymerization Through Reversible Chain Transfer between "Tight" and "Loose" Ion Pairs. *Angew. Chem., Int. Ed.* **2010**, *49*, 9140−9144. (b) Wei, J.; Hwang, W.; Zhang, W.; Sita, L. R. Dinuclear Bis-Propagators for the Stereoselective Living Coordinative Chain Transfer Polymerization of Propene. *J. Am. Chem. Soc.* **2013**, *135*, 2132−2135. (c) Wei, J.; Duman, L. M.; Redman, D. W.; Yonke, B. L.; Zavalij, P. Y.; Sita, L. R. N-Substituted Iminocaprolactams as Versatile and Low Cost Ligands in Group 4 Metal Initiators for the Living Coordinative Chain Transfer Polymerization of -Olefins. *Organometallics* **2017**, *36*, 4202−4207.

(17) Wei, J.; Zhang, W.; Sita, L. R. Aufbaureaktion Redux: Scalable Production of Precision Hydrocarbons from AlR_3 (R = Et or iBu) by Dialkyl Zinc Mediated Ternary Living Coordinative Chain-Transfer Polymerization. *Angew. Chem., Int. Ed.* **2010**, *49*, 1768−1772.

(18) Cueny, E. S.; Landis, C. R. Zinc-Mediated Chain Transfer from Hafnium to Aluminum in the Hafnium-Pyridyl Amido-Catalyzed Polymerization of 1-Octene Revealed by Job Plot Analysis. *Organometallics* **2019**, *38*, 926−932.

(19) (a) Thomas, T. S.; Hwang, W.; Sita, L. R. End-Group-Functionalized Poly(α-olefinates) as Non-Polar Building Blocks: Self-Assembly of Sugar−Polyolefin Hybrid Conjugates. *Angew. Chem., Int. Ed.* **2016**, *55*, 4683−4687. (b) Nowak, S. R.; Hwang, W.; Sita, L. R. Dynamic Sub-10-nm Nanostructured Ultrathin Films of Sugar-Polyolefin Conjugates Thermoresponsive at Physiological Temperatures. *J. Am. Chem. Soc.* **2017**, *139*, 5281−5284. (c) Lachmayr, K. K.; Wentz, C. M.; Sita, L. R. An Exceptionally Stable and Scalable Sugar-Polyolefin Frank-Kasper A15 Phase. *Angew. Chem., Int. Ed.* **2020**, *59*, 1521−1526. (d) Lachmayr, K. K.; Sita, L. R. Samall Molecule Modulation of Soft-Matter Frank-Kasper Phases: A Method for Adding Function to Form. *Angew. Chem., Int. Ed.* **2020**, *59*, 3563−3567.

(20) Britovsek, G. J. P.; Cohen, S. A.; Gibson, V. C.; Maddox, P. J.; van Meurs, M. Iron-Catalyzed Polyethylene Chain Growth on Zinc: Linear α-Olefins with a Poisson Distribution. *Angew. Chem., Int. Ed.* **2002**, *41*, 489−491.

(21) Britovsek, G. J. P.; Cohen, S. A.; Gibson, V. C.; van Meurs, M. Iron Catalyzed Polyethylene Chain Growth on Zinc: A Study of the Factors Delineating Chain Transfer versus Catalyzed Chain Growth in Zinc and Related Metal Alkyl Systems. *J. Am. Chem. Soc.* **2004**, *126*, 10701−10712.

(22) Thorshaug, K.; Støvneng, J. A.; Rytter, E.; Ystenes, M. Termination, Isomerization, and Propagation Reactions during Ethene Polymerization Catalyzed by Cp_2Zr-R+ and Cp^*_2Zr-R+. An Experimental and Theoretical Investigation. *Macromolecules* **1998**, *31*, 7149−7165.

(23) Chien, J. C. W.; Wang, B.-P. Metallocene-methylaluminoxane catalysts for olefin polymerization. V. Comparison of Cp_2ZrCl_2 and $CpZrCl_3$. *J. Polym. Sci., Part A: Polym. Chem.* **1990**, *28*, 15−38.

(24) Naga, N.; Mizunuma, K. Molecular weight and molecular weight distribution of polyethene obtained with rac-$Me_2Si(Ind)_2ZrCl_2$/methylaluminoxane. *Macromol. Chem. Phys.* **1998**, *199*, 113−118.

(25) D'Agnillo, L.; Soares, J. B. P.; Penlidis, A. Effect of operating conditions on the molecular weight distribution of polyethylene synthesized by soluble metallocene/methylaluminoxane catalysts. *Macromol. Chem. Phys.* **1998**, *199*, 955−962.

(26) Murtuza, S.; Casagrande, O. L.; Jordan, R. F. Ethylene Polymerization Behavior of Tris(pyrazolyl)borate Titanium(IV) Complexes. *Organometallics* **2002**, *21*, 1882−1890.

(27) Olonde, X.; Mortreux, A.; Petit, F.; Bujadoux, K. A useful method for the synthesis of neodymocene homogeneous catalysts for ethylene polymerization. *J. Mol. Catal.* **1993**, *82*, 75−82.

(28) Pelletier, J.-F.; Mortreux, A.; Olonde, X.; Bujadoux, K. Synthesis of New Dialkylmagnesium Compounds by Living Transfer Ethylene Oligo- and Polymerization with Lanthanocene Catalysts. *Angew. Chem., Int. Ed. Engl.* **1996**, *35*, 1854−1856.

(29) Pelletier, J. F.; Mortreux, A.; Petit, F.; Olonde, X.; Bujadoux, K. 23. Lanthanocene Based Catalysts for Olefin Polymerization: Scope and Present Limitations. *Stud. Surf. Sci. Catal.* **1994**, *89*, 249−256.

(30) Chenal, T.; Olonde, X.; Pelletier, J.-F.; Bujadoux, K.; Mortreux, A. Controlled polyethylene chain growth on magnesium catalyzed by lanthanidocene: A living transfer polymerization for the synthesis of higher dialkyl-magnesium. *Polymer* **2007**, *48*, 1844−1856.

(31) van Meurs, M.; Britovsek, G. J. P.; Gibson, V. C.; Cohen, S. A. Polyethylene Chain Growth on Zinc Catalyzed by Olefin Polymerization Catalysts: A Comparative Investigation of Highly Active Catalyst Systems across the Transition Series. *J. Am. Chem. Soc.* **2005**, *127*, 9913−9923.

(32) Arriola, D. J.; Carnahan, E. M.; Hustad, P. D.; Kuhlman, R. L.; Wenzel, T. T. Catalytic Production of Olefin Block Copolymers via Chain Shuttling Polymerization. *Science* **2006**, *312*, 714−719.

(33) Valente, A.; Mortreux, A.; Visseaux, M.; Zinck, P. Coordinative Chain Transfer Polymerization. *Chem. Rev.* **2013**, *113*, 3836−3857.

(34) Bochmann, M.; Lancaster, S. J. Monomer−Dimer Equilibria in Homo- and Heterodinuclear Cationic Alkylzirconium Complexes and Their Role in Polymerization Catalysis. *Angew. Chem., Int. Ed. Engl.* **1994**, *33*, 1634−1637.

(35) Bryliakov, K. P.; Talsi, E. P.; Voskoboynikov, A. Z.; Lancaster, S. J.; Bochmann, M. Formation and Structures of Hafnocene Complexes in MAO- and $AlBu^i_3/CPh_3[B(C_6F_5)_4]$-Activated Systems. *Organometallics* **2008**, *27*, 6333−6342.

(36) Camara, J. M.; Petros, R. A.; Norton, J. R. Zirconium-Catalyzed Carboalumination of α-Olefins and Chain Growth of Aluminum Alkyls: Kinetics and Mechanism. *J. Am. Chem. Soc.* **2011**, *133*, 5263−5273.

https://dx.doi.org/10.1021/acs.macromol.0c00552
Macromolecules 2020, 53, 5816−5825

(37) Petros, R. A.; Norton, J. R. Effectiveness in Catalyzing Carboalumination Can Be Inferred from the Rate of Dissociation of M/Al Dimers. *Organometallics* **2004**, *23*, 5105−5107.
(38) Cueny, E. S.; Johnson, H. C.; Anding, B. J.; Landis, C. R. Mechanistic Studies of Hafnium-Pyridyl Amido-Catalyzed 1-Octene Polymerization and Chain Transfer Using Quench-Labeling Methods. *J. Am. Chem. Soc.* **2017**, *139*, 11903−11912.
(39) Johnson, H. C.; Cueny, E. S.; Landis, C. R. Chain Transfer with Dialkyl Zinc During Hafnium−Pyridyl Amido-Catalyzed Polymerization of 1-Octene: Relative Rates, Reversibility, and Kinetic Models. *ACS Catal.* **2018**, *8*, 4178−4188.
(40) Cueny, E. S.; Johnson, H. C.; Landis, C. R. Selective Quench-Labeling of the Hafnium-Pyridyl Amido-Catalyzed Polymerization of 1-Octene in the Presence of Trialkyl-Aluminum Chain-Transfer Reagents. *ACS Catal.* **2018**, *8*, 11605−11614.
(41) Cueny, E. S.; Landis, C. R. The Hafnium-Pyridyl Amido-Catalyzed Copolymerization of Ethene and 1-Octene: How Small Amounts of Ethene Impact Catalysis. *ACS Catal.* **2019**, *9*, 3338−3348.
(42) Nelsen, D. L.; Anding, B. J.; Sawicki, J. L.; Christianson, M. D.; Arriola, D. J.; Landis, C. R. Chromophore Quench-Labeling: An Approach to Quantifying Catalyst Speciation As Demonstrated for (EBI)$ZrMe_2$/$B(C_6F_5)_3$-Catalyzed Polymerization of 1-Hexene. *ACS Catal.* **2016**, *6*, 7398−7408.
(43) Mayo, F. R. Chain Transfer in the Polymerization of Styrene: The Reaction of Solvents with Free Radicals1. *J. Am. Chem. Soc.* **1943**, *65*, 2324−2329.
(44) Hue, R. J.; Cibuzar, M. P.; Tonks, I. A. Analysis of Polymeryl Chain Transfer Between Group 10 Metals and Main Group Alkyls during Ethylene Polymerization. *ACS Catal.* **2014**, *4*, 4223−4231.
(45) Young, C. T.; von Goetze, R.; Tomov, A. K.; Zaccaria, F.; Britovsek, G. J. P. The Mathematics of Ethylene Oligomerisation and Polymerisation. *Top. Catal.* **2020**, DOI: 10.1007/s11244-019-01210-0.
(46) Rocchigiani, L.; Busico, V.; Pastore, A.; Talarico, G.; Macchioni, A. Unusual Hafnium−Pyridylamido/ERn Heterobimetallic Adducts (ERn = ZnR_2 or AlR_3). *Angew. Chem., Int. Ed.* **2014**, *53*, 2157−2161.

https://dx.doi.org/10.1021/acs.macromol.0c00552
Macromolecules 2020, 53, 5816−5825